arXiv:1606.05865v1 [hep-ph] 19 Jun 2016

Diphoton Resonance from a New Strong Force

Howard Georgi and Yuichiro Nakai

Department of Physics, Harvard University, Cambridge, MA 02138, USA

Abstract

We explore a "partial unification" model that could explain the diphoton event excess around 750 GeV recently reported by the LHC experiments. A new strong gauge group is combined with the ordinary color and hypercharge gauge groups. The VEV responsible for the combination is of the order of the $SU(2) \times U(1)$ breaking scale, but the coupling of the new physics to standard model particles is suppressed by the strong interaction of the new gauge group. This simple extension of the standard model has a rich phenomenology, including composite particles of the new confining gauge interaction, a coloron and a Z' which are rather weakly coupled to standard model particles, and massive vector bosons charged under both the ordinary color and hypercharge gauge groups and the new strong gauge group. The new scalar glueball could have mass of around 750 GeV, be produced by gluon fusion and decay into two photons, both through loops of the new massive vector bosons. The simplest version of the model has some issues: the massive vector bosons are stable and the coloron and the Z' are strongly constrained by search data. An extension of the model to include additional fermions with the new gauge coupling, though not as simple and elegant, can address both issues and more. It allows the massive vector boson to decay into a colorless, neutral state that could be a candidate of the dark matter. And the coloron and Z' can decay dominantly into the new fermions, completely changing the search bounds. In addition, $SU(N)$ fermions below the symmetry breaking scale make it more plausible that the lightest glueball is at 750 GeV. If the massive vector bosons are still long-lived, they could form new bound states, "vector bosoniums" with additional interesting phenomenology. Whatever becomes of the 750 GeV diphoton excess, the model is an unusual example of how new physics at small scales could be hidden by strong interactions.

1 Introduction

Recently, the ATLAS and CMS collaborations have reported an event excess in diphoton invariant mass distribution of around 750 GeV [1, 2]. If this excess is real and comes from a new scalar (or pseudoscalar) particle S decaying into two photons, the relatively large production cross section times branching ratio $\sigma(pp \to S)\mathrm{Br}(S \to \gamma\gamma)$ required to fit the data suggests a nonperturbatively large coupling of S with electrically charged particles and hence the existence of new strong dynamics (see e.g. Ref [3–6]).

In this paper, we report on an exercise in model building that is loosely motivated by the diphoton excess. We consider the possibility that this is a real effect from a previously unobserved strong gauge interaction. To connect the new strong dynamics with the diphoton excess, we pursue a "partial unification" scenario in which a part of the ordinary color and hypercharge gauge groups and the new strong gauge group are combined near the $SU(2) \times U(1)$-breaking scale of 250 GeV. We do not pretend that the structures we explore here are in any way unique and certainly not that they are well-motivated. But we do believe that it is interesting to build a very explicit and minimal model of such a scenario. This very simple extension of the standard model has a rich phenomenology at the TeV scale, including massive vector bosons which we call $X', \bar{X}'$, charged under both the ordinary color and hypercharge gauge groups and the new strong gauge group. The model also contains color octet vector bosons (colorons [7–9]) and a Z' (see for example [10]) both of which are rather weakly coupled to standard model particles, and color singlet and octet scalars (see for example [9]).

The lightest glueball associated with the new strong gauge interaction could be a scalar particle with mass of around 750 GeV.[1] This is natural in our model because all the other new states have masses that scale with the partial unification scale. The scale of confinement after the gauge symmetry breaking is generically smaller. The new scalar glueball is efficiently produced by gluon fusion and decays into two photons through loops of the new massive vector bosons $X', \bar{X}'$.

The simplest version of the model has some issues: the massive vector bosons are stable and the coloron and Z' are strongly constrained by search data. An extension of the model to include additional fermions, though not as simple and elegant, can address both issues and more. We show how this can allow the X' boson to decay into quarks and antiquarks plus a colorless, neutral state that could be an unusual dark matter candidate. The decays of the coloron and Z' into pairs of the new fermions are important in evading search constraints. There are many possible extensions of this kind, depending on the details of the partial unification. In the particular example we discuss in detail, the model contains one or more

[1] Ref [3] has discussed a glueball explanation for the diphoton excess in a different model.

charge 5/3 quarks and neutral fermions with the new strong interaction in a fairly narrow mass range from above 375 GeV (half the mass of the lightest glueball) to less than half the mass of the coloron. In addition, the $SU(N)$ fermions below the symmetry breaking scale make it more plausible that the lightest glueball is at 750 GeV.

Apart from the mass and decay constant of the lightest glueball, which we take from lattice gauge theory studies [11–13], the relevant spectrum and interactions in our model can be calculated perturbatively in some regions of the parameter space. However, as we will see, to explain the data, we will be pushed into a region of parameter space where the new gauge coupling is rather large, so some of our estimates may be only rough approximations, and indeed, we can't even be sure that the relevant symmetry breaking takes place as the perturbation theory suggests. Conversely, if the excess persists, and some scenario like this turns out to be the right explanation, we will learn a tremendous amount about strong gauge interactions that are very different from QCD.

The rest of the paper is organized as follows. In section 2, we present our model and analyze the mass spectra. We discuss some of the experimental constraints on the model in section 3. In section 4, we discuss the possibility that the lightest glueball associated with the new strong gauge interaction that is partially unified with color $SU(3)$ at a relatively low scale could explain the diphoton excess. In section 5, we add additional fermions to the model transforming under the new gauge interaction.

If the $X', \bar{X}'$ gauge bosons are still long-lived, they form new bound states, "vector bosoniums." Detailed phenomenology of the vector bosoniums is left for a future study. Various details including group theory notation and identities and some of the interactions in the model are relegated to appendices.

2 Partial unification

Here we discuss a minimal extension of the standard model in which a part of the color $SU(3)$ and the hypercharge $U(1)$ resides in an extended gauge group. The $U(1)$ normalization is important for determining the electric charge of the new massive vector bosons. In this section, we describe the symmetry breaking in detail and analyze the mass spectra of the scalar fields and the vector bosons.

2.1 The $SU(N+3)$ model

We introduce a new $SU(N+3)_H$ gauge theory with a complex scalar ξ which is charged under both the $SU(N+3)_H$ gauge group and the (would-be) standard model gauge groups $SU(3)_{C'} \times U(1)_{Y'}$. The charge assignment is shown in Table 1. Thus the ξ transforms like

	$SU(N+3)_H$	$SU(3)_{C'}$	$SU(2)_L$	$U(1)_{Y'}$
ξ	$\mathbf{N+3}$	$\bar{\mathbf{3}}$	$\mathbf{1}$	$-\frac{Nq}{N+3}$

Table 1: The charge assignment of the ξ field. The $U(1)_{Y'}$ charge of ξ is explained in the main text.

	Gauge field	Gauge coupling	Generator
$SU(N+3)_H$	H_μ^A	g_H	T^A
$SU(3)_{C'}$	A'^a_μ	g'_3	T^a
$SU(2)_L$	W_μ^α	g_2	T^α
$U(1)_{Y'}$	B'_μ	g'_Y	$S_{Y'}$

Table 2: The names of gauge fields, gauge couplings and generators of the model. Here, $A = 1, \cdots, (N+3)^2 - 1$, $a = 1, \cdots, 8$ and $\alpha = 1, 2, 3$. More group theory notation and identities are summarized in appendix A.

$(N+3, \bar{3})_{-Nq/(N+3)}$ under $SU(N+3)_H \times SU(3)_{C'} \times U(1)_{Y'}$ and it is convenient to represent it as an $(N+3) \times 3$ matrix. The names of gauge fields, gauge couplings and generators are summarized in Table 2. The ordinary standard model particles have the conventional charges under the $SU(3)_{C'} \times SU(2)_L \times U(1)_{Y'}$. We can also introduce new matter fermions charged under the $SU(N+3)_H$ gauge group, which have an interesting role in the massive gauge boson decay. This will be discussed in section 5. The most general potential involving only the scalar ξ can be written as

$$V_\xi = \frac{1}{4}\lambda_1 \left(\mathrm{Tr}(\xi^\dagger \xi) - 3a^2\right)^2 + \frac{1}{2}\lambda_2 \,\mathrm{Tr}\left(\xi^\dagger \xi - a^2 I_3\right)^2 , \tag{2.1}$$

where I_3 is the 3×3 identity matrix, λ_1, λ_2 are dimensionless parameters and a is a mass parameter.

For the range of parameters

$$\lambda_2 > 0 \,, \qquad \lambda_1 > -\frac{2}{3}\lambda_2 \,, \tag{2.2}$$

the potential (2.1) is minimized when some of the components in ξ get nonzero vacuum

	$SU(N)_H$	$SU(3)_C$	$SU(2)_L$	$U(1)_Y$
X'	$\overline{\mathbf{N}}$	$\mathbf{3}$	$\mathbf{1}$	q
$\bar{X}'$	$\mathbf{N}$	$\bar{\mathbf{3}}$	$\mathbf{1}$	$-q$
Z'	$\mathbf{1}$	$\mathbf{1}$	$\mathbf{1}$	0
G'	$\mathbf{1}$	$\mathbf{8}$	$\mathbf{1}$	0

Table 3: The charge assignments of the massive vector bosons.

expectation values. The vev can be put in the following form

$$\langle \xi \rangle = \begin{pmatrix} a & 0 & 0 \\ 0 & a & 0 \\ 0 & 0 & a \\ 0 & 0 & 0 \\ \vdots & \vdots & \vdots \end{pmatrix} , \tag{2.3}$$

and the gauge groups $SU(N+3)_H \times SU(3)_{C'} \times SU(2)_L \times U(1)_{Y'}$ are spontaneously broken to $SU(N)_H \times SU(3)_C \times SU(2)_L \times U(1)_Y$. Below the scale a, the gauge structure is just the conventional standard model with an additional $SU(N)$ gauge group that does not couple to the standard model particles. Thus for a large a the gauge couplings of the $SU(3)_C \times SU(2)_L \times U(1)_Y$ would be just the standard model couplings to a good approximation. However, we will see that this is not an interesting limit. Instead, we will be interested in a of the order of (or even smaller than) the $SU(2) \times U(1)$ breaking scale $v \approx 250$ GeV. We will try to convince you of the somewhat surprising statement that such a low value of a is not ruled out by current data. Roughly speaking, this works because the heavy gauge boson masses are of the order of a times a large coupling g_H, and in many cases can be integrated out as if a were large. In general, this is a dangerous procedure, because the large coupling can appear in the numerator and spoil decoupling. But here is it often OK, because there are no direct order-g_H couplings to the standard model particles.

The model contains massive particles whose masses scale with a. Corresponding to the broken symmetries, there are massive $X', \bar{X}'$ gauge bosons, charged under both $SU(3)_C$, $U(1)_Y$ and the new $SU(N)_H$, as well as the Z' and the color octet G' vector bosons. The G' gauge boson is also called as the coloron. The charge assignments of the massive vector bosons are summarized in Table 3. In this mass range, there are also massive scalars, G_O and G_S transforming like an octet and singlet respectively under the color $SU(3)_C$. Their mass spectra are analyzed below.

2.2 Gauge couplings

After the symmetry breaking, the ordinary $SU(3)_C$, $U(1)_Y$ gauge groups are given by combinations of the $SU(N+3)_H$ gauge group and the $SU(3)_{C'}$, $U(1)_{Y'}$ gauge groups. The ordinary massless gluons and their gauge coupling g_s are given by the following relations,

$$A_\mu^a = \frac{g_3' H_\mu^a + g_H A_\mu'^a}{\sqrt{g_H^2 + (g_3')^2}}\,, \qquad \frac{1}{g_s^2} = \frac{1}{(g_H)^2} + \frac{1}{(g_3')^2}\,, \tag{2.4}$$

where g_H and g_3' are the gauge couplings of the $SU(N+3)_H$ and $SU(3)_{C'}$ gauge groups respectively. The field H_μ^a $(a = 1, \cdots, 8)$ is the $SU(3)$ part of the $SU(N+3)_H$ gauge field H_μ^A $(A = 1, \cdots, (N+3)^2 - 1)$.

We next consider the $U(1)$ normalization. The $U(1)_{Y'}$ charge of ξ is given by $-N/(N+3)$ times the $U(1)_Y$ charge of the X' gauge boson, which we call q. The $U(1)$ subgroup of $SU(N+3)_H$ commuting with the $SU(3)$ and $SU(N)$ subgroups, is generated by

$$S_H \equiv \frac{q}{N+3}\begin{pmatrix} N\, I_3 & 0 \\ 0 & -3\, I_N \end{pmatrix}\,, \qquad [S_H, T_{3\times N}] = 0\,, \qquad T_{3\times N} = \begin{pmatrix} T_3 & 0 \\ 0 & T_N \end{pmatrix}\,, \tag{2.5}$$

which is normalized so that the $U(1)_Y$ charge of the standard model is given by

$$S_Y = S_H + S_{Y'}\,. \tag{2.6}$$

In this case, we correctly obtain $S_Y\langle\xi\rangle = 0$, which means S_Y is not broken in the effective theory between the scale a and the Higgs vev. On the other hand, the properly normalized generator of the $U(1)$ subgroup is

$$\tilde{S}_H = k S_H\,, \qquad k = \frac{\sqrt{N+3}}{q\sqrt{6N}}\,. \tag{2.7}$$

Note that because the $SU(N+3)_H$ does not involve the electroweak $SU(2)_L$, there is no constraint on the X' charge q from the structure of the electroweak interactions. However, if we require that states that are singlets under the color $SU(3)_C$ and the confining $SU(N)_H$ are integrally charged, then we have the constraint

$$\begin{aligned} q &= \frac{3j-1}{3N} \quad \text{for integer } j \text{ if } N \bmod 3 = 1\,, \\ q &= \frac{3j+1}{3N} \quad \text{for integer } j \text{ if } N \bmod 3 = 2\,, \\ q &= \frac{j}{N} \quad \text{for integer } j \text{ if } N \bmod 3 = 0\,. \end{aligned} \tag{2.8}$$

Another constraint on q is discussed below.

The ordinary massless hypercharge gauge field B_μ and its gauge coupling g_Y are given by

$$B_\mu = \frac{g'_Y B''_\mu + g''_Y B'_\mu}{\sqrt{(g'_Y)^2 + (g''_Y)^2}}\,, \qquad \frac{1}{g_Y^2} = \frac{1}{(g'_Y)^2} + \frac{1}{(g''_Y)^2}\,, \tag{2.9}$$

where

$$g''_Y = k g_H\,, \qquad k = \frac{\sqrt{N+3}}{q\sqrt{6N}}\,, \tag{2.10}$$

and B''_μ is the (properly normalized) $U(1)$ part of the $SU(N+3)_H$ gauge field. Because the low energy theory is identical to the standard model as $a \to \infty$, this implies that to leading order in $(v/a)^2$ (v is the Higgs vev)

$$\frac{1}{\sqrt{1/(k g_H)^2 + 1/(g'_Y)^2}} \simeq \frac{e}{\cos\theta_W}\,. \tag{2.11}$$

Here, $\sin^2\theta_W = 0.23$ is the weak mixing angle and e is the electromagnetic gauge coupling. Solving this equation for g'_Y, we obtain

$$g'_Y \simeq \frac{1}{\sqrt{\frac{\cos^2\theta_W}{e^2} - \frac{6Nq^2}{(N+3)g_H^2}}}\,, \tag{2.12}$$

which implies that q cannot be too large.

2.3 Massive vector bosons

We here analyze the mass spectrum of the G', Z' and X', $\bar{X}'$ gauge bosons and some of their interactions. From the covariant derivative of the scalar ξ which has the vev (2.3), the coloron G' and the massive vector boson corresponding to the broken $U(1)$ are given by the linear combinations,

$$G'^a_\mu = \frac{g_H H^a_\mu - g'_3 A'^a_\mu}{\sqrt{g_H^2 + (g'_3)^2}}\,, \qquad B^-_\mu = \frac{g''_Y B''_\mu - g'_Y B'_\mu}{\sqrt{(g'_Y)^2 + (g''_Y)^2}}\,. \tag{2.13}$$

The vector boson masses are

$$\begin{aligned} m^2_{G'} &= a^2\left(g_H^2 + (g'_3)^2\right)\,, \\ m^2_{B^-} &= 6\left(\frac{Nq}{N+3}\right)^2 a^2\left((g'_Y)^2 + (g''_Y)^2\right)\,, \\ m^2_{X'} &= g_H^2 a^2\,. \end{aligned} \tag{2.14}$$

Note that the coloron is always heavier than the X', $\bar{X}'$ gauge bosons.

After $SU(2) \times U(1)$ breaking, the massless photon field is the linear combination,

$$A_\mu = \frac{g_Y W_\mu^3 + g_2 B_\mu}{\sqrt{(g_2)^2 + (g_Y)^2}} \,. \tag{2.15}$$

The two massive eigenstates are given by

$$Z_\mu = \cos\omega \hat{Z}_\mu + \sin\omega B_\mu^- \,, \qquad Z'_\mu = -\sin\omega \hat{Z}_\mu + \cos\omega B_\mu^- \,, \tag{2.16}$$

where

$$\hat{Z}_\mu = \frac{g_2 W_\mu^3 - g_Y B_\mu}{\sqrt{(g_2)^2 + (g_Y)^2}} \,, \qquad \tan 2\omega = -2\frac{\delta\hat{m}^2}{\hat{m}_{B^-}^2 - \hat{m}_Z^2} \,, \tag{2.17}$$

and

$$\begin{aligned} \hat{m}_Z^2 &= \frac{1}{4} v^2 \left((g_2)^2 + (g_Y)^2 \right) \,, \\ \hat{m}_{B^-}^2 &= \frac{1}{4} v^2 \frac{(g'_Y)^4}{(g'_Y)^2 + (g''_Y)^2} + m_{B^-}^2 \,, \\ \delta\hat{m}^2 &= \frac{1}{4} v^2 (g'_Y)^2 \frac{\sqrt{(g_2)^2 + (g_Y)^2}}{\sqrt{(g'_Y)^2 + (g''_Y)^2}} \,. \end{aligned} \tag{2.18}$$

The eigenvalues are

$$\begin{aligned} m_Z^2 &= \frac{1}{2}\left(\hat{m}_Z^2 + \hat{m}_{B^-}^2 - \sqrt{\left(\hat{m}_Z^2 - \hat{m}_{B^-}^2\right)^2 + 4\delta\hat{m}^4} \right) \,, \\ m_{Z'}^2 &= \frac{1}{2}\left(\hat{m}_Z^2 + \hat{m}_{B^-}^2 + \sqrt{\left(\hat{m}_Z^2 - \hat{m}_{B^-}^2\right)^2 + 4\delta\hat{m}^4} \right) \,. \end{aligned} \tag{2.19}$$

We now summarize the interactions of the massive gauge bosons with the standard model fermion f for later purposes. The $X', \bar{X}'$ gauge bosons do not couple to the standard model fermion at tree level. The coloron interaction with the standard model fermion is

$$\mathcal{L} \supset -\frac{(g'_3)^2}{\sqrt{g_H^2 + (g'_3)^2}} \, \bar{f}\gamma^\mu T^a f \, G''^a_\mu \,. \tag{2.20}$$

The important point is that the coupling is small when the g_H coupling is large. This will be the interesting region for our analysis. In this region, $g'_3 \approx g_s$ by the relation (2.4).

The Z' couplings are more complicated because the $SU(2)$ symmetry breaking scale v is important. Even though we will keep the new symmetry breaking scale, a, of the same order as v, because the strong $SU(N+3)$ group is not directly coupled to standard model particles, we will be able to expand quantities in $1/g_H$ to simplify our expressions and understand what is going on. At leading order in $1/g_H$, the masses satisfy

$$g_H a \approx m_{G'} \approx m_{X'} \approx \sqrt{\frac{N+3}{N}} m_{Z'} \tag{2.21}$$

and the Z' interaction is

$$\mathcal{L} \supset -\sqrt{\frac{6Nq}{(N+3)}} \frac{(g'_Y)^2}{g_H} \left(Y_L^f \bar{f}_L \gamma^\mu f_L + Y_R^f \bar{f}_R \gamma^\mu f_R \right) Z'_\mu \,. \tag{2.22}$$

Here, $Y_{L,R}^f$ are the hypercharges of the left and right-handed fermions $f_{L,R}$. Again the interaction is suppressed when the g_H coupling is large and $g'_Y \approx e/\cos\theta_W$ by the relation (2.9).

2.4 Scalar mass spectrum

The scalar ξ has $6(N+3)$ (real) degrees of freedom. Here, $8+1+6N$ of them are unphysical Nambu-Goldstone modes eaten in the symmetry breaking. Thus there are 9 physical degrees of freedom. The potential of the scalar sector is given by (2.1) plus terms involving the standard model Higgs ϕ,

$$V_{\text{Higgs}} = \frac{1}{4}\lambda_3 \left(\phi^\dagger \phi - \frac{v^2}{2} \right)^2 + \lambda_4 \left(\phi^\dagger \phi - \frac{v^2}{2} \right) \left(\text{Tr}(\xi^\dagger \xi) - 3a^2 \right) , \tag{2.23}$$

where λ_3 and λ_4 are dimensionless coupling constants. To analyze the mass spectrum of the physical modes, we now take unitary gauge,

$$\xi = \begin{pmatrix} aI_3 + \chi/\sqrt{2} \\ 0 \end{pmatrix} , \qquad \phi = \frac{1}{\sqrt{2}} \begin{pmatrix} 0 \\ v+h \end{pmatrix} , \qquad \text{where } \chi^\dagger = \chi \,. \tag{2.24}$$

The trace and traceless parts of χ are singlet and octet under the color $SU(3)_C$ respectively. Properly normalizing the kinetic terms, the color octet/singlet scalars are written (using the Gell-Mann matrices λ^a) as

$$G_O^a = \text{Tr}\,(\lambda^a \chi) \,, \qquad G_S \equiv \sqrt{\frac{2}{3}} \text{Tr}\,(\chi) \tag{2.25}$$

Then, the mass of the octet scalar G_O is given by

$$m_{G_O}^2 = 2\lambda_2 a^2 \,. \tag{2.26}$$

Due to the second term of (2.23), the singlet component G_S mixes with the Higgs field h. The mass eigenstates are

$$\phi_1 = h\cos\theta_h + G_S \sin\theta_h \,, \qquad \phi_2 = -h\sin\theta_h + G_S\cos\theta_h \,. \tag{2.27}$$

The mixing angle θ_h is given by

$$\tan 2\theta_h = -\frac{2\sqrt{6}\lambda_4 v a}{m_{G_S}^2 - m_h^2} \,, \tag{2.28}$$

where

$$m_{G_S}^2 = \left(3\lambda_1 + \frac{2}{3}\lambda_2\right) a^2 \,, \qquad m_h^2 = \frac{1}{2}\lambda_3 v^2 \,. \tag{2.29}$$

The eigenvalues are

$$\begin{aligned} m_{\phi_1}^2 &= \frac{1}{2}\left(m_h^2 + m_{G_S}^2\right) - \frac{1}{2}\sqrt{\left(-m_h^2 + m_{G_S}^2\right)^2 + 24\lambda_4^2 v^2 a^2} \,, \\ m_{\phi_2}^2 &= \frac{1}{2}\left(m_h^2 + m_{G_S}^2\right) + \frac{1}{2}\sqrt{\left(-m_h^2 + m_{G_S}^2\right)^2 + 24\lambda_4^2 v^2 a^2} \,. \end{aligned} \tag{2.30}$$

The mass of the lighter eigenstate m_{ϕ_1} gives the physical Higgs boson mass, $m_{\phi_1} \simeq 125\,\mathrm{GeV}$.

3 Experimental constraints

In this section, we discuss the experimental constraints on the new parameters that we have introduced in our extension of the standard model. The possible constraints are of three kinds. There are constraints from precise tests of the standard model at low energies. There are "conpositeness" constraints on the virtual effects of the new particles. In addition, there are bounds from direct searches for the new particles in our model, in particular the lower bounds on the Z' mass and the coloron mass.

3.1 Electroweak precision tests

For a sufficiently large a, the low-energy interactions of the standard model particles are indistinguishable from their standard model limits. But our a will not be large, so precise

tests of the standard model create interesting constraints. Let us consider the $U(1)$ part of the model,

$$\mathcal{L} \supset -\frac{1}{4}B'_{\mu\nu}B'^{\mu\nu} - \frac{1}{4}B''_{\mu\nu}B''^{\mu\nu} + \frac{1}{2}m^2_{B^-}B^-_\mu B^{-\mu}\,. \tag{3.1}$$

Here, $B'_{\mu\nu}$ and $B''_{\mu\nu}$ are the field strengths of the B'_μ and B''_μ gauge fields respectively. The B'_μ field couples to the usual standard model fields with the gauge coupling g'_Y. We can integrate out the heavy mode at tree level by solving the equation of motion for the B''_μ field, given by

$$\partial^\nu B''_{\mu\nu} - m^2_{B''}B''_\mu = -\frac{g'_Y}{g''_Y}m^2_{B''}B'_\mu\,, \qquad m^2_{B''} \equiv \left(\frac{(g''_Y)^2}{(g'_Y)^2+(g''_Y)^2}\right)m^2_{B^-}\,. \tag{3.2}$$

We have defined a handy parameter $m^2_{B''}$ which is not a physical mass. This equation of motion has a solution,

$$B''_{\mu\nu} = \frac{g'_Y}{g''_Y}\frac{\delta^\nu_\mu + \partial_\mu\partial^\nu/m^2_{B''}}{1+\partial^2/m^2_{B''}}B'_\nu\,. \tag{3.3}$$

Thus the Lagrangian after integrating out B''_μ at tree level is given by

$$\begin{aligned}\mathcal{L}_{\text{eff}} &\supset -\frac{1}{4}B'_{\mu\nu}B'^{\mu\nu} - \frac{1}{4}\left(\frac{g'_Y}{g''_Y}\right)^2 B'_{\mu\nu}\left(\frac{1}{1+\partial^2/m^2_{B''}}\right)B'^{\mu\nu} \\ &= -\frac{1}{4}\frac{(g'_Y)^2+(g''_Y)^2}{(g''_Y)^2}B'_{\mu\nu}B'^{\mu\nu} + \frac{1}{4}\left(\frac{g'_Y}{g''_Y}\right)^2 B'_{\mu\nu}\left(\frac{\partial^2}{m^2_{B''}}\right)B'^{\mu\nu} + \cdots\,.\end{aligned} \tag{3.4}$$

We have omitted to write irrelevant dimension eight and higher operators. Correctly normalizing the kinetic term as in (2.9), we obtain

$$\mathcal{L}_{\text{eff}} \supset -\frac{1}{4}B_{\mu\nu}B^{\mu\nu} - \frac{1}{4}\left(\frac{g'_Y}{g''_Y}\right)^2\frac{1}{m^2_{B^-}}(\partial_\rho B^{\mu\nu})^2 + \cdots\,, \tag{3.5}$$

where B_μ is the ordinary hypercharge gauge field which couples to the standard model fields with the gauge coupling g_Y. Note that there are no effective operators to give the S, T and U parameters [14]. However, the second term of this Lagrangian contributes to the so-called Y parameter [15],

$$Y = \left(\frac{g'_Y}{g''_Y}\frac{m_W}{m_{B^-}}\right)^2 \simeq \left(\frac{g'_Y}{g''_Y}\frac{m_W}{m_{Z'}}\right)^2\,, \tag{3.6}$$

where m_W is the W boson mass. The direct constraint on the Y parameter is $Y = (4.2 \pm 4.9)\times 10^{-3}$. Note that a similar analysis applies in any model with a Z' which mixes only through the $U(1)$.

3.2 The Z' mass bound

The Z' boson is mainly produced by Drell-Yan like quark annihilation at the LHC. This boson can decay into a pair of leptons. The null result of dielectron and dimuon final state searches by the ATLAS and CMS detectors [16, 17] gives the strongest bound on the Z' mass. From the interaction (2.22), the decay width of Z' into a pair of fermions is given by

$$\Gamma(Z' \to f\bar{f}) = \frac{C_f m_{Z'}}{24\pi} \frac{(g'_Y)^4}{(g'_Y)^2 + (g''_Y)^2} \left((Y_L^f)^2 + (Y_R^f)^2 \right) , \tag{3.7}$$

where C_f is the color factor (1 for a color singlet and 3 for a color triplet). The Z' boson can also decay into two bosons, $Z' \to W^+W^-, Zh, ZG_S$, if kinematically allowed. These are not dominant in the most of the parameter space and do not dramatically affect the branching ratio into leptons. The coupling (2.22) also implies the Drell-Yan production rate of the Z' is inversely proportional to g_H^2 for large g_H. But this does not help much. If the Z' decays dominantly into standard model particles, the branching ratio into leptons is large and a Z' lighter than a few TeV is ruled out [18, 19]. However, if we introduce new fermions charged under the $SU(N+3)_H$ gauge group, as we do in section 5, the coupling of the Z' to these is proportional to g_H, and therefore much larger than the coupling to standard model particles. If the Z' decay into these fermions is kinematically allowed, it dominates over the standard model decays in the interesting region of large g_H and a light Z' is not impossible.

3.3 Coloron phenomenology

Let us look at the color octet massive vector bosons, colorons, which are also mainly produced by quark annihilation at the LHC. The NLO cross section of coloron production from quark annihilation has been calculated in Ref [20]. The gluon fusion contribution has been analyzed in Ref [21] and gives a sub-leading effect. The coloron can decay into $G_O G_O$, $G_O Z'$, $q\bar{q}$ and $X'\bar{X}'$ if these decay modes are open. The relevant interactions of these decay modes are summarized in appendix B.1. The two-body decay rates of the coloron are then given by

$$\begin{aligned}
\Gamma(G' \to G_O G_O) &= \frac{1}{256\pi} \frac{\left(g_H^2 - (g'_3)^2\right)^2}{g_H^2 + (g'_3)^2} m_{G'} \left(1 - \frac{4m_{G_O}^2}{m_{G'}^2}\right)^{3/2} , \\
\Gamma(G' \to G_O Z') &= \frac{1}{36\pi} \left(g_H^2 + (g'_3)^2\right) \frac{m_{Z'}^2}{m_{G'}^2} \mathbf{p} \left(3 + \frac{\mathbf{p}^2}{m_{Z'}^2}\right) , \\
\Gamma(G' \to q\bar{q}) &= \frac{1}{24\pi} \frac{(g'_3)^4}{g_H^2 + (g'_3)^2} m_{G'} \left(1 - \frac{4m_q^2}{m_{G'}^2}\right)^{1/2} ,
\end{aligned}$$

$$\Gamma(G' \to X'\bar{X}') = \frac{N}{96\pi} \frac{g_H^4}{g_H^2 + (g_3')^2} m_{G'} \left(1 - \frac{4m_{X'}^2}{m_{G'}^2}\right)^{3/2} \left(3 - \frac{m_{G'}^2}{m_{X'}^2} + \frac{m_{G'}^4}{4m_{X'}^4}\right) , \tag{3.8}$$

where m_q is the quark mass and

$$\mathbf{p}^2 = \frac{1}{4m_{G'}^2} \left(m_{G'}^2 - (m_{Z'} - m_{G_O})^2\right) \left(m_{G'}^2 - (m_{Z'} + m_{G_O})^2\right) . \tag{3.9}$$

Because of (2.21), we do not expect the $G' \to X'\bar{X}'$ to be allowed in the interesting region of large g_H. As in the case of the Z' boson, if we introduce new fermions charged under the $SU(N+3)_H$ gauge group, G' can also decay into the quark components of the new fermions. Because the $m_{Z'} < m_{G'}$ for large g_H (by (2.21) again), the coloron decay is kinematically allowed whenever the Z' decay is. Thus if we introduce new $SU(N+3)$ fermions to evade the Z' search bounds, we will automaatically evade the coloron search bounds. If the G_O is very light, the $G' \to G_O G_O$ mode and perhaps $G' \to G_O Z'$ can be important.

Another experimental constraint on the coloron mass and its interactions with the standard model quarks comes from searches for quark contact interactions. The coloron exchange induces four-fermion interactions among the quarks,

$$\mathcal{L}_{\text{eff}} \supset -\frac{(g_3')^4}{g_H^2 + (g_3')^2} \frac{1}{m_{G'}^2} \left(\bar{q}\gamma_\mu T^a q\right) \left(\bar{q}\gamma^\mu T^a q\right) . \tag{3.10}$$

These quark contact interactions lead to constructive interference with the ordinary QCD terms and hence deviation of dijet angular distributions from the perturbative QCD predictions.

There is certainly a strong constraint on (3.10) from LHC data. Unfortunately, the published results from CMS in [22] consider only a set of contact terms which they call "the most general flavor diagonal" set, but which is not general enough to include (3.10). This poor choice also appears in the particle data group review of compositeness [23]. A sensible general form appears in [24], but unfortunately this does not seem to have been universally adopted in the literature. We expect that the constraint on (3.10) will be of the same order of magnitude of those quoted in [22].

$$a = \frac{m_{G'}}{\sqrt{g_H^2 + (g_3')^2}} \gtrapprox \frac{(g_3')^2}{g_H^2 + (g_3')^2} \, 5 \text{ TeV} \tag{3.11}$$

This constraint is not affected (at least not very much) by the additional $SU(N+3)$ fermions that we will introduce in section 5.

Note that this constraint gives a very severe lower bound on the scale a in the small g_H region of our parameter space because the coloron mass is approximately given by $m_{G'} \approx g_3' a$ in this region. But for large g_H, relatively light colorons may be allowed.

4 N-Glueballs and the 750 GeV diphoton excess

We here consider phenomenology of the glueballs associated with the $SU(N)_H$ gauge theory, which we call N-glueballs, and their possible explanation of the 750 GeV diphoton excess observed at the LHC. First, we discuss the mass spectrum of the N-glueballs. Then, we analyze the effective higher dimensional operators involving N-gluons and the standard model particles which are relevant for the glueball decays. We find a region of parameter space where the lightest glueball at around 750 GeV could explain the diphoton excess while satisfying the experimental constraints discussed above. The decays of the pseudoscalar and spin 2 glueballs are also presented.

4.1 The N-glueball masses

Below the scale of the $SU(N+3)_H$ symmetry breaking, the unbroken $SU(N)_H$ gauge interaction becomes strong and finally confines giving rise to the N-glueball spectrum. For very small g_H coupling, the confinement scale of the $SU(N)_H$ pure Yang-Mills gauge theory, denoted as Λ_H, is generically well below the symmetry breaking scale, and we can estimate it using 0-loop matching and the 1-loop β-function:

$$\Lambda_H = m_{X'}\, e^{-\frac{6\pi}{(11N-2n_f)\alpha_H(a)}}\,. \tag{4.1}$$

Here, $\alpha_H(a) \equiv g_H^2(a)/4\pi$ means the gauge coupling at the scale a and n_f is the number of $SU(N)$ fermions in the low-energy theory. Note that the confinement scale is scheme independent at 1-loop level. We could improve on (4.1) using the techniques of Hall and Weinberg [25, 26] including 1-loop matching and 2-loop renormalization, but this will not change the qualitative message of (4.1). Λ_H is smaller than $m_{X'}$, but for large α_H, we would expect the exponential factor in (4.1) to be of order 1 unless the running in the low-energy theory is very slow, for example by having matter fields to nearly cancel the effect of $SU(N)_H$ gauge fields.

For a given Λ_H, we can appeal to lattice calculations to estimate the glueball masses. From [12], the scalar glueball 0^{++} is the lightest and its mass m_0 is estimated to lie in the region $4.7\Lambda^{\overline{MS}} < m_0 < 11\Lambda^{\overline{MS}}$ ($\Lambda^{\overline{MS}}$ is the $\overline{MS}$ scheme confinement scale) with very small dependence on N. From the lattice result [11], the spin 2^{++} glueball mass is $m_{2^{++}} \simeq 1.4\, m_0$ and the pseudoscalar glueball mass is $m_{0^{-+}} \simeq 1.5\, m_0$. There are many other states but we concentrate on these three lightest N-glueballs in the rest of the discussion.

As we have seen in the discussion of experimental constraints, and will emphasize below, the interesting parameter space that might explain the diphoton excess is in large α_H region. In this region, our theory is strongly coupled and (4.1) is certainly a reliable quantitative

J^{PC}	Operator
0^{++}	$S = \mathrm{Tr}\, F_{\mu\nu}F^{\mu\nu}$
0^{-+}	$P = \mathrm{Tr}\, F_{\mu\nu}\tilde{F}^{\mu\nu}$
2^{++}, 1^{-+}, 0^{++}	$T_{\mu\rho} = \mathrm{Tr}\, F_{\mu\lambda}F_{\rho}{}^{\lambda} - \frac{1}{4}g_{\mu\rho}S$
2^{++}, 2^{-+}	$L_{\mu\nu\rho\sigma} = \mathrm{Tr}\, F_{\mu\nu}F_{\rho\sigma} - \frac{1}{2}\left(g_{\mu\rho}T_{\nu\sigma} + g_{\nu\sigma}T_{\mu\rho} - g_{\mu\sigma}T_{\nu\rho} - g_{\nu\rho}T_{\mu\sigma}\right)$ $-\frac{1}{12}\left(g_{\mu\rho}g_{\nu\sigma} - g_{\mu\sigma}g_{\nu\rho}\right)S + \frac{1}{12}\epsilon_{\mu\nu\rho\sigma}P$

Table 4: The dimension four operator which represents each glueball state. Here, $F_{\mu\nu}$ denotes the field strength of the $SU(N)_H$ gauge boson and $\tilde{F}_{\mu\nu} = \frac{1}{2}\epsilon_{\mu\nu\rho\sigma}F^{\rho\sigma}$. The trace acts on the $SU(N)_H$ generators.

J^{PC}	Operator
1^{--}, 1^{+-}	$\Omega^{(1)}_{\mu\nu} = \mathrm{Tr}\, F_{\mu\nu}F_{\rho\sigma}F^{\rho\sigma}$
1^{--}, 1^{+-}	$\Omega^{(2)}_{\mu\nu} = \mathrm{Tr}\, F_{\mu}{}^{\rho}F_{\rho}{}^{\sigma}F_{\sigma\nu}$

Table 5: The dimension six operator which represents each glueball state.

guide. It is even unclear that the relevant symmetry breaking takes place as the perturbation theory suggests. Thus, we do not know the relation between the X' mass and the glueball mass. We will simply assume that the X' mass and the glueball mass are of the same order and in the interesting region for the diphoton excess.

4.2 The dimension eight operators

In our model, the N-glueballs can decay into the standard model gauge bosons through loops of the $X', \bar{X}'$ gauge bosons. When the confinement scale Λ_H is sufficiently small compared to the scale a, the situation is similar to the so-called Hidden Valley scenario [27] where the $X', \bar{X}'$ gauge bosons correspond to mediators between the standard model sector and the hidden $SU(N)_H$ gauge sector. Ref [28] has discussed the hidden glueball decays into the standard model gauge bosons through loops of heavy fermions. In ref [28], these decays are analyzed using the factorized matrix elements,

$$\begin{aligned}\mathcal{M}(\Psi \to \mathcal{A}\mathcal{A}) &= \langle SM|\mathcal{O}_{SM}|0\rangle\langle 0|\mathcal{O}_H|\Psi\rangle\,,\\ \mathcal{M}(\Psi \to \Psi' + \mathcal{A}) &= \langle SM|\mathcal{O}_{SM}|0\rangle\langle \Psi'|\mathcal{O}_H|\Psi\rangle\,.\end{aligned} \tag{4.2}$$

Here, $\Psi^{(\prime)}$ denotes a glueball state and $\mathcal{A}$ the standard model gauge bosons collectively. After integrating out heavy fields in the loops, the decays are described by dimension eight operators, $\mathcal{L}_{\rm eff} \supset \mathcal{O}_{SM}\mathcal{O}_H$ where $\mathcal{O}_{SM}$ represents an operator composed of the standard model gauge fields. Table 4 (5) shows the relevant dimension four (six) operator $\mathcal{O}_H$ which represents each glueball state [13, 28]. Then, the effective Lagrangian after integrating out the $X', \bar{X}'$ gauge bosons can be written as

$$\begin{aligned}\mathcal{L}_{\rm eff} = &\frac{g_H^2}{(4\pi)^2 m_{X'}^4}\left(g_Y^2\kappa_Y B^{\mu\nu}B^{\rho\sigma} + g_s^2\kappa_s \mathrm{Tr}\, G^{\mu\nu}G^{\rho\sigma}\right)\\ &\times\left(a_S S g_{\mu\rho}g_{\nu\sigma} + a_P P\epsilon_{\mu\nu\rho\sigma} + a_T T_{\mu\rho}g_{\nu\sigma} + a_L L_{\mu\nu\rho\sigma}\right)\\ &+\frac{g_H^3 g_Y}{(4\pi)^2 m_{X'}^4}\kappa_\Omega\left(b_1 B^{\mu\nu}\Omega^{(1)}_{\mu\nu} + b_2 B^{\mu\nu}\Omega^{(2)}_{\mu\nu}\right),\end{aligned} \tag{4.3}$$

where $B_{\mu\nu}$ and $G_{\mu\nu}$ denote the field strengths of the ordinary hypercharge and color gauge fields and $\kappa_Y = 6q^2$, $\kappa_s = 2$ and $\kappa_\Omega = 6q$. The coefficients $a_{S,P,T,L}$, $b_{1,2}$ are obtained by the one-loop computation. Two examples of the relevant diagrams of the $X', \bar{X}'$ gauge boson loops are shown in Figure 1. The calculation of the coefficients has been done in [29, 30] and is summarized in appendix C. The results are

$$\begin{aligned}&a_S = \frac{89}{480}, \qquad a_P = \frac{79}{960}, \qquad a_T = \frac{7}{5}, \qquad a_L = \frac{1}{40},\\ &b_1 = -\frac{5}{16}, \qquad b_2 = \frac{27}{20}.\end{aligned} \tag{4.4}$$

The coefficient a_S here is about a factor of ten larger than when particles inside the loops are fermions ($a_S|_{\rm fermion} = 1/60$ [28]). Thus the production cross section of the lightest glueball by gluon fusion is enhanced by a factor of $\mathcal{O}(100)$. This is one of the promising features in this model for the explanation of the reported diphoton excess.

4.3 The scalar effective operator

The mixing between the scalar N-glueball and the singlet scalar G_S is generated by loops of the $X', \bar{X}'$ gauge bosons. This may be important for the glueball decays because the singlet G_S also mixes with the Higgs boson and the glueball decays into a pair of the standard model fermions and massive gauge bosons are induced through these mixings. The one-loop diagrams of the massive vector boson X' to generate the effective interaction of the $SU(N)_H$ gauge fields with G_S are shown in Figure 2 (There are also the diagrams of the $\bar{X}'$ gauge boson). The relevant interactions of the $X', \bar{X}'$ gauge bosons with the scalar G_S and the $SU(N)_H$ gauge fields are summarized in appendix B.2. The similar calculation as the case of

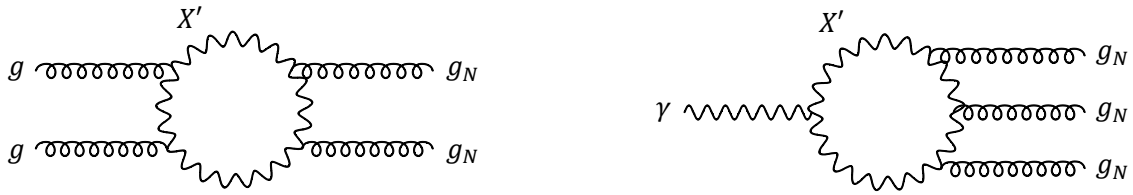

Figure 1: Two example diagrams of the $X', \bar{X}'$ gauge boson loops to generate the effective dimension eight operators of the N-glueballs with the standard model gauge fields. Here, g, γ and g_N denote the ordinary gluon, the photon and the $SU(N)_H$ gauge boson respectively.

the Higgs boson decays through the W boson loops gives the mixing term between G_S and the scalar glueball,

$$\mathcal{L}_{G_S-S} = \frac{\alpha_H}{2\pi}\frac{k_{g_N}}{\Lambda_{g_N}} G_S\, S\,, \qquad \frac{k_{g_N}}{\Lambda_{g_N}} = -\left(\frac{3}{4\sqrt{6}a}\right) F_V(\tau_{X'})\,. \tag{4.5}$$

Here, we have defined $\tau_{X'} \equiv m_{G_S}^2/(4m_{X'}^2)$. The loop function $F_V(\tau)$ is given by

$$F_V(\tau) = -\left(\tau^{-1}(3+2\tau) + 3\tau^{-2}(-1+2\tau)Z(\tau)\right)\,, \tag{4.6}$$

and

$$Z(\tau) = \begin{cases} \left[\sin^{-1}(\sqrt{\tau})\right]^2 & (\tau \le 1) \\ -\frac{1}{4}\log\left[\frac{1+\sqrt{1-\tau^{-1}}}{1-\sqrt{1-\tau^{-1}}} - i\pi\right]^2 & (\tau \ge 1) \end{cases}\,. \tag{4.7}$$

Using this effective interaction, we will discuss the lightest N-glueball decays into a pair of the standard model fermions and massive gauge bosons.

We here comment on phenomenology of the singlet scalar G_S briefly. The G_S scalar can be produced by gluon fusion through loops of both the coloron and the $X', \bar{X}'$ gauge bosons. The produced G_S decays into a pair of the standard model gauge bosons and the Higgs bosons. The decays into the standard model fermions and massive gauge bosons are also possible through the mixing with the Higgs boson. Furthermore, when the mass of G_S is larger than twice the N-glueball mass, the same loops of the $X', \bar{X}'$ gauge bosons as above induce the G_S decay into two glueballs. We leave detailed phenomenology of the scalar G_S to a future study.

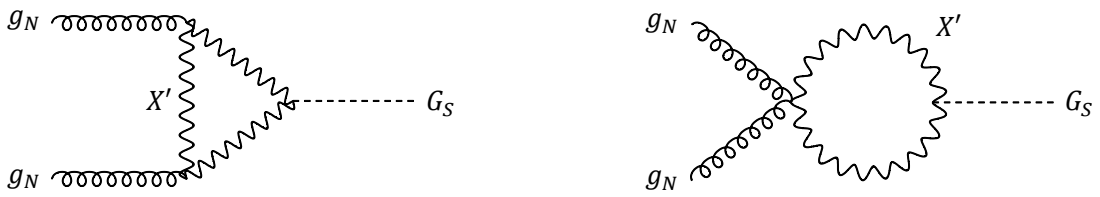

Figure 2: One-loop diagrams of the X' gauge boson to contribute to the effective interaction of the $SU(N)_H$ gauge fields with the color singlet scalar G_S. There are also the diagrams of the $\bar{X}'$ gauge boson.

4.4 The lightest glueball decays

We now consider the decays of the lightest N-glueball 0^{++} through the effective dimension eight operators in (4.3) generated by loops of the $X', \bar{X}'$ vector bosons. The glueball dominantly decays into a pair of gluons. The diphoton decay is also induced by the new vector boson loops. As discussed above, the decay amplitude is written by the factorized matrix element (4.2). The amplitude of the glueball decay into a pair of gluons is then given by

$$\mathcal{M}(0^{++} \to gg) = \frac{\alpha_s \alpha_H}{m_{X'}^4} \kappa_s a_S \, \langle g_1^a g_2^b | \mathrm{Tr}\, G_{\mu\nu} G^{\mu\nu} | 0 \rangle \langle 0 | S | 0^{++} \rangle \,. \tag{4.8}$$

Here, the transition to two gluons is $\langle g_1^a g_2^b | \mathrm{Tr}\, G_{\mu\nu} G^{\mu\nu} | 0 \rangle = \delta^{ab} \left(k_\mu^1 \epsilon_\nu^1 - k_\nu^1 \epsilon_\mu^1 \right) (k^{2\mu} \epsilon^{2\nu} - k^{2\nu} \epsilon^{2\mu})$ where $k^{1,2}$ are gluon momenta and $\epsilon^{1,2}$ are polarizations. From this decay amplitude, the decay rate is calculated as

$$\Gamma(0^{++} \to gg) = \frac{8 \alpha_s^2 \alpha_H^2}{16 \pi m_{X'}^8} \kappa_s^2 a_S^2 m_0^3 \left(\mathbf{F}^{\mathbf{S}}_{\mathbf{0}^{++}} \right)^2 \,, \tag{4.9}$$

where $\mathbf{F}^{\mathbf{S}}_{\mathbf{0}^{++}} \equiv \langle 0 | S | 0^{++} \rangle$ is the decay constant of the scalar glueball 0^{++} and $2.00\, m_0^3 \leq 4\pi \alpha_H \mathbf{F}^{\mathbf{S}}_{\mathbf{0}^{++}} \leq 4.77\, m_0^3$ from the lattice result for the $SU(3)$ pure Yang-Mills theory [12]. We assume that this lattice result persists also in cases with general numbers of N. In the same way, we can compute the decay rates of $0^{++} \to \gamma\gamma, ZZ, Z\gamma$. The branching ratios are given by

$$\mathrm{Br}(0^{++} \to \gamma\gamma) \simeq \frac{\Gamma(0^{++} \to \gamma\gamma)}{\Gamma(0^{++} \to gg)} = \frac{\alpha^2}{2\alpha_s^2} \frac{\kappa_Y^2}{\kappa_s^2} = \frac{9}{2} \frac{q^4 \alpha^2}{\alpha_s^2} \,, \tag{4.10}$$

and

$$\mathrm{Br}(0^{++}\to ZZ)\simeq\frac{\Gamma(0^{++}\to ZZ)}{\Gamma(0^{++}\to gg)}=\frac{\alpha^2\tan^4\theta_W}{2\alpha_s^2}\frac{\kappa_Y^2}{\kappa_s^2}\left(1-\frac{4m_Z^2}{m_0^2}\right)^{1/2}\left(1-\frac{4m_Z^2}{m_0^2}+\frac{6m_Z^4}{m_0^4}\right),$$
$$\mathrm{Br}(0^{++}\to Z\gamma)\simeq\frac{\Gamma(0^{++}\to Z\gamma)}{\Gamma(0^{++}\to gg)}=\frac{\alpha^2\tan^2\theta_W}{\alpha_s^2}\frac{\kappa_Y^2}{\kappa_s^2}\left(1-\frac{m_Z^2}{m_0^2}\right)^3. \tag{4.11}$$

Here, we have assumed that the total decay width is approximately given by $\Gamma_{\rm total}\simeq\Gamma(0^{++}\to gg)$. These decay modes are also induced through the glueball mixing with the G_S scalar but they are effectively two-loop effects and can be ignored. Note that the branching ratio of the diphoton decay is completely determined by the electric charge q of the X' gauge boson unlike the case where particles in the loops are various fermions with various masses and charges.

From the mixing term (4.5) generated by loops of the $X',\bar{X}'$ gauge bosons, the glueball decays $0^{++}\to hh, f\bar{f}, WW$ are also possible. The decays $G_S\to hh, f\bar{f}, WW$ are induced by the G_S interaction and mixing with the Higgs boson. All of these depend on the coupling λ_4 that governs G_S-h mixing, so they need not be large. At leading order in λ_4, the decay rates of $0^{++}\to hh, f\bar{f}, WW$ are written as

$$\begin{aligned}
\Gamma(0^{++}\to hh)&=\left(\frac{2\alpha_H k_{g_N}\mathbf{F}^{\mathbf{S}}_{\mathbf{0}^{++}}}{4\pi\Lambda_{g_N}(m_{G_S}^2-m_0^2)}\right)^2\Gamma_{G_S\to hh}(m_0^2)\\
&\simeq\left(\frac{2\alpha_H k_{g_N}\mathbf{F}^{\mathbf{S}}_{\mathbf{0}^{++}}}{4\pi\Lambda_{g_N}(m_{G_S}^2-m_0^2)}\right)^2\frac{\left(\sqrt{6}\lambda_4 a/2\right)^2}{32\pi m_0}\sqrt{1-\frac{4m_h^2}{m_0^2}},\\
\Gamma(0^{++}\to f\bar{f})&=\left(\frac{2\alpha_H k_{g_N}\mathbf{F}^{\mathbf{S}}_{\mathbf{0}^{++}}}{4\pi\Lambda_{g_N}(m_{G_S}^2-m_0^2)}\right)^2\Gamma_{G_S\to f\bar{f}}(m_0^2)\\
&\simeq\left(\frac{2\alpha_H k_{g_N}\mathbf{F}^{\mathbf{S}}_{\mathbf{0}^{++}}}{4\pi\Lambda_{g_N}(m_{G_S}^2-m_0^2)}\right)^2\left(\frac{3\sqrt{6}\,\lambda_4}{9\lambda_1+2\lambda_2}\frac{v}{a}\right)^2\Gamma^{\rm SM}_{h\to f\bar{f}}(m_0^2),\\
\Gamma(0^{++}\to WW)&=\left(\frac{2\alpha_H k_{g_N}\mathbf{F}^{\mathbf{S}}_{\mathbf{0}^{++}}}{4\pi\Lambda_{g_N}(m_{G_S}^2-m_0^2)}\right)^2\Gamma_{G_S\to WW}(m_0^2)\\
&\simeq\left(\frac{2\alpha_H k_{g_N}\mathbf{F}^{\mathbf{S}}_{\mathbf{0}^{++}}}{4\pi\Lambda_{g_N}(m_{G_S}^2-m_0^2)}\right)^2\left(\frac{3\sqrt{6}\,\lambda_4}{9\lambda_1+2\lambda_2}\frac{v}{a}\right)^2\Gamma^{\rm SM}_{h\to WW}(m_0^2).
\end{aligned}\tag{4.12}$$

Here, $\Gamma_{h\to f\bar{f}}(m_0^2)$ and $\Gamma_{h\to WW}(m_0^2)$ are the decay rates of the Higgs boson into a pair of the standard model fermions and the W bosons evaluated at the mass scale of the glueball. The

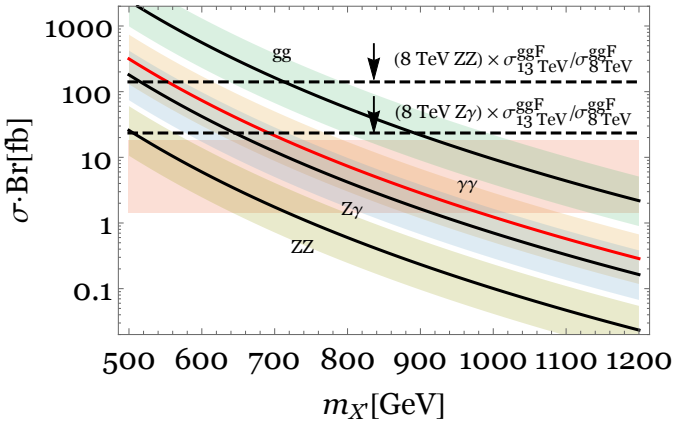

Figure 3: The production cross section times branching ratio $\sigma(pp \to 0^{++})\,\mathrm{Br}(0^{++} \to \gamma\gamma)$ at the $\sqrt{s} = 13\,\mathrm{TeV}$ LHC. We take the electric charge of the X' gauge boson as $q = 5/3$. The resonance searches in ZZ [31] and $Z(\to \ell\ell)\gamma$ [18] at $\sqrt{s} = 8\,\mathrm{TeV}$ rescaled by the ratio $\sigma^{\mathrm{ggF}}_{13\,\mathrm{TeV}}/\sigma^{\mathrm{ggF}}_{8\,\mathrm{TeV}} \simeq 4.7$ put upper bounds on the production cross section times branching ratios. Uncertainty of the glueball decay constant $\mathbf{F}^{\mathbf{S}}_{\mathbf{0}^{++}}$ is included in each line (which corresponds to $4\pi\alpha_H \mathbf{F}^{\mathbf{S}}_{\mathbf{0}^{++}} = 3.12\, m_0^3$). The observed diphoton excess can be explained with $640\,\mathrm{GeV} \lesssim m_{X'} \lesssim 1100\,\mathrm{GeV}$.

branching ratios of these decay modes depend on the parameters of the scalar sector. In the rest of the discussion, we assume the λ_4 coupling is not too large (or the G_S scalar is heavy) so that they do not dominate over the diphoton decay.

The present calculations of the glueball decay rates only take into account the leading order effects. At the next-to-leading order, we have substantial α_s and α_H corrections. Then, the actual total decay rate of the lightest N-glueball may be larger.

4.5 The diphoton excess

Now we can put everything together and discuss the possibility that the lightest N-glueball 0^{++} explains an event excess in diphoton invariant mass distribution of around 750 GeV reported by the ATLAS and CMS collaborations [1, 2]. The glueball can be produced by gluon fusion through the effective dimension eight operator in (4.3) generated by loops of the $X', \bar{X}'$ vector bosons. With the narrow width approximation [32, 33], the production cross section times branching ratio $\sigma(pp \to 0^{++})\,\mathrm{Br}(0^{++} \to \gamma\gamma)$ is expressed as

$$\begin{aligned}\sigma(pp \to 0^{++})\,\mathrm{Br}(0^{++} \to \gamma\gamma) \simeq{}& \frac{\pi^2}{8 m_0 s}\,\Gamma(0^{++} \to \gamma\gamma) \\ &\times \int_0^1 dx_1 \int_0^1 dx_2 \left[\delta(x_1 x_2 - m_0^2/s) g(x_1) g(x_2)\right] ,\end{aligned} \tag{4.13}$$

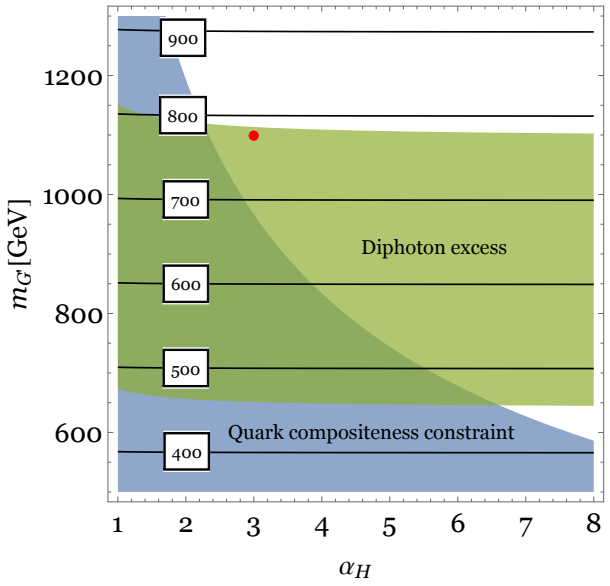

Figure 4: The region of α_H and the coloron mass $m_{G'}$ which can explain the reported diphoton excess (the green band). Here, we assume $N = 3$ and $q = 5/3$. The blue shaded region is not allowed from the constraint on the quark compositeness constraint. The Y parameter constraint is weak in this parameter region. The model-dependent direct bounds on the Z' mass and the coloron mass are not ahown. Although we do not know the precise mass relation between the coloron and the glueballs for large α_H, we assume that the lightest glueball mass is at 750 GeV in the region which can explain the diphoton excess. The red dot denotes a benchmark point mentioned in the main text.

where s is the square of center of mass energy and $g(x)$ is the parton distribution function (PDF) of the gluon. We have assumed $\Gamma_{\rm total} \simeq \Gamma(0^{++} \to gg)$. From (4.9) and (4.10), we can calculate $\sigma(pp \to 0^{++})\,{\rm Br}(0^{++} \to \gamma\gamma)$ with $m_0 = 750\,{\rm GeV}$. By using MSTW PDF [34], this is numerically given by

$$\sigma(pp \to 0^{++})\,{\rm Br}(0^{++} \to \gamma\gamma) \simeq 2.9\,{\rm fb} \times \left(\frac{q}{5/3}\right)^4 \left(\frac{m_{X'}}{900\,{\rm GeV}}\right)^{-8} \quad (\sqrt{s} = 13\,{\rm TeV})\,. \tag{4.14}$$

The reported excess at $\sqrt{s} = 13\,{\rm TeV}$ is [4]

$$1.4\,{\rm fb} \lesssim \sigma(pp \to 0^{++})\,{\rm Br}(0^{++} \to \gamma\gamma) \lesssim 18\,{\rm fb}\,. \tag{4.15}$$

Figure 3 shows the production cross section times branching ratio $\sigma(pp \to 0^{++})\,{\rm Br}(0^{++} \to \gamma\gamma)$ at the $\sqrt{s} = 13\,{\rm TeV}$ LHC. The shaded region denotes the observed excess. We take the electric charge of the X' gauge boson as $q = 5/3$. The resonance searches in ZZ [31] and $Z(\to \ell\ell)\gamma$ [18] at $\sqrt{s} = 8\,{\rm TeV}$ rescaled by the ratio $\sigma^{\rm ggF}_{13\,{\rm TeV}}/\sigma^{\rm ggF}_{8\,{\rm TeV}} \simeq 4.7$ put upper bounds

on the production cross section times branching ratios. Uncertainty of the glueball decay constant $\mathbf{F}^{\mathbf{S}}_{\mathbf{0}^{++}}$ is included in each line (which corresponds to $4\pi\alpha_H \mathbf{F}^{\mathbf{S}}_{\mathbf{0}^{++}} = 3.12\, m_0^3$). The observed diphoton excess can be explained with $640\,\text{GeV} \lesssim m_{X'} \lesssim 1100\,\text{GeV}$. As the charge q is large, the upper bound on the X' mass is relaxed as far as the upper bound on q from (2.12) is satisfied.

We now look at the model parameter space where the experimental constraints are satisfied and the diphoton excess can be explained. Figure 4 shows the region of α_H and the coloron mass $m_{G'}$ which can explain the reported diphoton excess (the green band). Here, we assume $N = 3$ and $q = 5/3$. The blue shaded region is not allowed from the constraint on the quark contact interaction induced from the coloron exchange (3.11). We can see that, as expected, this constraint pushes the interesting parameter space to the large α_H region. The Y parameter constraint is weak in this region. The model-dependent search bounds on the Z' mass and the coloron mass are not shown, but are weak if the Z' boson and the coloron decay into new fermions. Although we do not know the precise relation between the coloron mass and the glueball mass for large α_H, we assume that the lightest glueball mass is at 750 GeV in the interesting parameter region that can explain the diphoton excess.

An interesting benchmark point, shown in figure 4 (red dot), is $\alpha_H = 3$ and $m_{G'} = 1100$ GeV. This gives $m_{Z'} \approx 777$ GeV, $m_{X'} \approx 1083$ GeV. For this choice of parameter, $SU(N+3)$ fermions with mass between 375 GeV and $m_{Z'}/2$ can dominate the Z' and coloron decay widths.

4.6 The pseudoscalar glueball decays

We next consider the decays of the pseudoscalar N-glueball 0^{-+} through the effective dimension eight operator (4.3). As in the case of the lightest scalar glueball, the width of the pseudoscalar glueball decay into a pair of gluons is

$$\Gamma(0^{-+} \to gg) = \frac{8\alpha_s^2 \alpha_H^2}{16\pi m_{X'}^8} \kappa_s^2 a_P^2 m_{0^{-+}}^3 \left(\mathbf{F}^{\mathbf{P}}_{\mathbf{0}^{-+}}\right)^2 , \tag{4.16}$$

where $\mathbf{F}^{\mathbf{P}}_{\mathbf{0}^{-+}} \equiv \langle 0|P|0^{-+}\rangle$ is the decay constant of the pseudoscalar glueball. We can also compute the decay rates of $0^{-+} \to \gamma\gamma, ZZ, Z\gamma$. The branching ratios are given by

$$\text{Br}(0^{-+} \to \gamma\gamma) \simeq \frac{\Gamma(0^{-+} \to \gamma\gamma)}{\Gamma(0^{-+} \to gg)} = \frac{\alpha^2}{2\alpha_s^2}\frac{\kappa_Y^2}{\kappa_s^2} = \frac{9}{2}\frac{q^4\alpha^2}{\alpha_s^2} ,$$

$$\text{Br}(0^{-+} \to ZZ) \simeq \frac{\Gamma(0^{-+} \to ZZ)}{\Gamma(0^{-+} \to gg)} = \frac{\alpha^2 \tan^4\theta_W}{2\alpha_s^2}\frac{\kappa_Y^2}{\kappa_s^2}\left(1 - \frac{4m_Z^2}{m_{0^{-+}}^2}\right)^{3/2} ,$$

$$\mathrm{Br}(0^{-+}\to Z\gamma)\simeq\frac{\Gamma(0^{-+}\to Z\gamma)}{\Gamma(0^{-+}\to gg)}=\frac{\alpha^2\tan^2\theta_W}{\alpha_s^2}\frac{\kappa_Y^2}{\kappa_s^2}\left(1-\frac{m_Z^2}{m_{0^{-+}}^2}\right)^3 . \tag{4.17}$$

The pseudoscalar glueball can also decay into the lightest glueball with a pair of gauge bosons, but its branching ratio is significantly suppressed, as discussed in Ref [28].

When we fix the scalar glueball mass at $m_0 = 750\,\mathrm{GeV}$, the mass of the pseudoscalar glueball is $m_{0^{-+}} \simeq 1.1\,\mathrm{TeV}$. Numerically, the ratios are then calculated as

$$\begin{aligned}&\mathrm{Br}(0^{-+}\to gg):\mathrm{Br}(0^{-+}\to\gamma\gamma):\mathrm{Br}(0^{-+}\to ZZ):\mathrm{Br}(0^{-+}\to Z\gamma)\\&\simeq 1-0.028\,q^4:0.017\,q^4:0.0015\,q^4:0.010\,q^4 .\end{aligned} \tag{4.18}$$

The branching ratios of $0^{-+}\to\gamma\gamma, Z\gamma$ are the same with those of the scalar glueball decays. The decay to two gluons is dominant and the diphoton decay is the next. The existence of this particle is one of the predictions in the glueball scenario of the reported diphoton excess.

4.7 The 2^{++} glueball decays

Finally, we summarize the decays of the 2^{++} N-glueball. The existence of this glueball is also a prediction in the present scenario. The decay rates of $2^{++}\to gg,\gamma\gamma,ZZ,Z\gamma$ are calculated in Ref [28] for the case where particles inside the loops are fermions. They are expressed in terms of the decay constants of the 2^{++} glueball,

$$\begin{aligned}&\langle 0|T_{\mu\nu}|2^{++}\rangle\equiv\mathbf{F}^{\mathbf{T}}_{\mathbf{2}^{++}}\epsilon_{\mu\nu}\,,\\&\langle 0|L_{\mu\nu\rho\sigma}|2^{++}\rangle\equiv\mathbf{F}^{\mathbf{L}}_{\mathbf{2}^{++}}\left(\mathcal{P}_{\mu\rho}\epsilon_{\nu\sigma}-\mathcal{P}_{\mu\sigma}\epsilon_{\nu\rho}+\mathcal{P}_{\nu\sigma}\epsilon_{\mu\rho}-\mathcal{P}_{\nu\rho}\epsilon_{\mu\sigma}\right)\,.\end{aligned} \tag{4.19}$$

Here, $\epsilon_{\mu\nu}$ is the polarization tensor of 2^{++} and $\mathcal{P}_{\mu\nu}\equiv g_{\mu\nu}-2p_\mu p_\nu/p^2$. The results of the decay rates are given by

$$\Gamma(2^{++}\to gg)=\frac{8\alpha_s^2\alpha_H^2}{160\pi m_{X'}^8}\kappa_s^2 m_{2^{++}}^3\left(\frac{1}{2}a_T^2\left(\mathbf{F}^{\mathbf{T}}_{\mathbf{2}^{++}}\right)^2+\frac{4}{3}a_L^2\left(\mathbf{F}^{\mathbf{L}}_{\mathbf{2}^{++}}\right)^2\right),$$

$$\Gamma(2^{++}\to\gamma\gamma)=\frac{4\alpha^2\alpha_H^2}{160\pi m_{X'}^8}\kappa_Y^2 m_{2^{++}}^3\left(\frac{1}{2}a_T^2\left(\mathbf{F}^{\mathbf{T}}_{\mathbf{2}^{++}}\right)^2+\frac{4}{3}a_L^2\left(\mathbf{F}^{\mathbf{L}}_{\mathbf{2}^{++}}\right)^2\right),$$

$$\begin{aligned}\Gamma(2^{++}\to ZZ)=\frac{\alpha^2\alpha_H^2\tan^4\theta_W}{40\pi m_{X'}^8}\kappa_Y^2 m_{2^{++}}^3\left(1-4x_2\right)^{1/2}\Bigg(&\frac{1}{2}a_T^2 f_T(x_2)\left(\mathbf{F}^{\mathbf{T}}_{\mathbf{2}^{++}}\right)^2\\&+\frac{4}{3}a_L^2 f_L(x_2)\left(\mathbf{F}^{\mathbf{L}}_{\mathbf{2}^{++}}\right)^2+\frac{40}{3}a_T a_L f_{TL}(x_2)\,\mathbf{F}^{\mathbf{T}}_{\mathbf{2}^{++}}\mathbf{F}^{\mathbf{L}}_{\mathbf{2}^{++}}\Bigg),\end{aligned}$$

	$SU(N+3)_H$	$SU(3)_{C'}$	$SU(2)_L$	$U(1)_{Y'}$
ψ	$\mathbf{N+3}$	$\mathbf{1}$	$\mathbf{1}$	$\frac{3q}{N+3}$

Table 6: The charge assignment of the fermion relevant to the X' decay.

	$SU(N)_H$	$SU(3)_C$	$SU(2)_L$	$U(1)_Y$
χ	$\mathbf{N}$	$\mathbf{1}$	$\mathbf{1}$	0
η	$\mathbf{1}$	$\mathbf{3}$	$\mathbf{1}$	q

Table 7: The charge assignment of the fermion $\psi = (\chi, \eta)$ after the symmetry breaking.

$$\Gamma(2^{++} \to Z\gamma) = \frac{\alpha^2 \alpha_H^2 \tan^2\theta_W}{20\pi m_{X'}^8} \kappa_Y^2 m_{2^{++}}^3 (1-x_2)^3 \left(\frac{1}{2} a_T^2 g_T(x_2) \left(\mathbf{F^T_{2^{++}}}\right)^2 + \frac{4}{3} a_L^2 g_L(x_2) \left(\mathbf{F^L_{2^{++}}}\right)^2 + \frac{20}{3} a_T a_L x_2 \, \mathbf{F^T_{2^{++}}} \mathbf{F^L_{2^{++}}} \right), \tag{4.20}$$

where $x_2 = m_Z^2/m_{2^{++}}^2$ and

$$\begin{aligned} &f_T(x) = 1 - 3x + 6x^2\,, \quad f_L(x) = 1 + 2x + 36x^2\,, \quad f_{TL}(x) = x(1-x)\,, \\ &g_T(x) = 1 + \frac{1}{2}x + \frac{1}{6}x^2\,, \quad g_L(x) = 1 + 3x + 6x^2\,. \end{aligned} \tag{4.21}$$

When we fix the scalar glueball mass at $m_0 = 750\,\mathrm{GeV}$, the mass of the spin 2 glueball $m_{2^{++}}$ is around 1 TeV.

5 The X' decay

In the simplest version of the model that we have discussed above, there is an unbroken $U(1)$ global symmetry under which the $X', \bar{X}'$ gauge bosons are charged and hence these massive gauge bosons are stable. While this is not obviously ruled out experimentally and cosmologically (at least if the reheating temperature after inflation is sufficiently low and also non-thermal production of the $X', \bar{X}'$ gauge bosons is suppressed), we here comment on a modest extension of the model which allows the X' boson to decay without breaking the $U(1)$ global symmetry.

Let us introduce a Dirac fermion ψ charged under the $U(1)_{Y'}$ gauge group and the $SU(N+3)_H$ gauge group with a Dirac mass between 375 GeV and $m_{Z'}/2$. Table 6 and Table 7 show the charge assignments of this fermion $\psi = (\chi, \eta)$ before and after the symmetry breaking.

The χ and η components are approximately degenerate because there are no renormalizable couplings of ψ to the ξ field. We assume that the new fermion interacts with the standard model matter fields. The possible interaction depends on the charge q of the X' gauge boson. For instance, when the charge is $q = 5/3$, we can write down (for example) the following invariant non-renormalizable interaction term (in Majorana notation):

$$\frac{1}{M_{UV}^3}(u_R^{j_3}\beta u_R^{k_3})(d_{j_3L}^c\beta\psi_{j_NL}^c)\xi_{k_3}^{j_N} + \text{h.c.} \tag{5.1}$$

where u_R and d_R are the ordinary right-handed up and down quarks, j_3 and k_3 are color indices and j_N is an $SU(N)_H$ index, all summed over. Then, if the X' gauge boson is heavier than the χ, it can decay as follows:

$$X' \to \bar{\chi}u\bar{u}\bar{d}\,. \tag{5.2}$$

The electrically neutral fermion χ is stable and might be a candidate of the dark matter.

The colored fermion η can be produced at the LHC but its collider phenomenology significantly depends on its charge and the details of its decays. For example, for $q = 5/3$, η is a charge 5/3 quark and the interaction term (5.1) along with the ξ VEV produces the decay

$$\eta \to u\bar{u}\bar{d}\,. \tag{5.3}$$

If the lifetime of this fermion is long enough, the pair produced $\eta\bar{\eta}$ may form a bound state like charmonium. If the decay (5.3) is fast, we may see the $u\bar{u}\bar{d}$ jets in the LHC detectors. The detailed analysis is beyond the scope of this paper and will be discussed elsewhere.

If the scale M_{UV} is very low, we may worry that the UV completion will include flavor-changing netural-current effects. It is interesting to note that we can generalize (5.1) to incorporate a $SU(3)_U \times SU(3)_D$ symmetry acting on the right handed charge 2/3 and charge $-1/3$ quarks respectively. The generalization, now including $SU(3)_U$ flavor indices, j_U, k_U and ℓ_U and a $SU(3)_D$ flavor index j_D (again all summed over), looks like

$$\frac{1}{M_{UV}^3}(U_R^{j_3j_U}\beta U_R^{k_3k_U})\epsilon_{j_Uk_U\ell_U}(D_{j_3j_DL}^c\beta\psi_{j_NL}^{c\ell_Uj_D})\xi_{k_3}^{j_N} + \text{h.c.} \tag{5.4}$$

Now we have nine ψ fields which carry the U and D flavor symmetries (and it is amusing to note that this is getting close to the number of $SU(N)$ fermions necessary slow the running of the $SU(N)$ coupling below the $m_{X'}$ scale). Thus we can tune the coupling to preserve the flavor symmetry. Likewise, we can adjust things so that the Dirac mass terms for the ψ fermions are equal, preserving the symmetry. None of this is natural but it suggests that the flavor changing neutral currents will not be an insurmountable constraint, even if the coupling is fairly strong.

6 Conclusion

In this paper, we have described a partial unification model that could explain the reported diphoton event excess. A part of the color $SU(3)$ and the hypercharge $U(1)$ resides in an extended gauge group that is broken by a VEV **slightly smaller than the Higgs VEV!** We have discussed the experimental constraints on the new parameters. Precise tests of the standard model at low energies constrain the model parameters and require the coupling of the new gauge group to be large. Constraints from searches for the Z' and the coloron require that they decay dominantly into new particles. The scalar glueball associated with the new confining gauge theory can have a mass of around 750 GeV and be produced by gluon fusion and decay into two photons through loops of the new massive vector bosons $X, \bar{X}'$. The production and decays are analyzed by the effective dimension eight operator of the glueball and the mixing term with the singlet scalar. We have found a parameter space where this glueball could explain the diphoton excess. The decays of the pseudoscalar and spin 2 glueballs have been also presented.

One of the important predictions in the present model is the existence of the $X', \bar{X}'$ gauge bosons, which may be pair produced at colliders. In the simplest version of the model, the $X', \bar{X}'$ gauge bosons are stable. We have discussed a modest extension of the model which allows the X' boson to decay into a colorless, neutral fermion. The lifetime of the X' gauge boson depends on the mass of the new fermion and the size of the coupling of the interaction term with the standard model field(s) like (5.1). When the X' gauge boson is stable at collider time scales, the bound states of the $X', \bar{X}'$ gauge bosons, the vector bosoniums, are formed. When the reported diphoton excess is explained in the present model, the mass of the lightest vector bosonium is predicted at around 2 TeV. Detailed phenomenology of the vector bosoniums is left for a future study. It might be also interesting to clarify whether a stable baryonic bound state of the neutral fermion could give the correct dark matter abundance.

Our model is neither natural nor beautiful, but we believe it is instructive. We close by reiterating a few of the things we have noticed from the analysis that may be more generally useful.

- A partial unification not involving the electroweak $SU(2)$ can depend on an arbitrary charge, q (see (2.5) and the discussion following).

- "Flavor-diagonality" is an inappropriate assumption for compositeness tests (see (3.10) and the discussion following).

- Perhaps the most important and surprising message is that a low partial unification scale with new particles that have large mass because their couplings to the symmetry

breaking field are large may be only weakly constrained if the strong interactions do not directly involve the standard model fermions (see (3.6) and the discussion following).

Thus even if (as seems likely) the reported diphoton excess at 750 GeV is washed away in a flood of new data, we believe that we have learned something. Our model is an explicit example of how new physics could be hidden right in front of our noses at the $SU(2) \times U(1)$ breaking scale and below.

Acknowledgments

We would like to thank Prateek Agrawal, Masaki Asano, Tatsuhiko Ikeda, Matthew Reece, Ryosuke Sato and Matthew Strassler for fruitful discussions. We are particularly grateful to M. Reece for many important comments from the very beginning of this work. HG is supported in part by the National Science Foundation under grant PHY-1418114. YN is supported by a JSPS Fellowship for Research Abroad.

A Normalization and identities of group theory

We here summarize normalization and identities of $SU(N+3)$ and its subgroups. The commutation relations are

$$[T^A, T^B] = i f^{ABC} T^C \,, \tag{A.1}$$

where T^A $(A = 1, \cdots, (N+3)^2 - 1)$ are generators and f^{ABC} are totally antisymmetric structure constants. The anti-commutation relations are

$$\{T^A, T^B\} = \delta^{AB} \frac{\mathbf{1}}{N+3} + d^{ABC} T^C \,, \tag{A.2}$$

where d^{ABC} are totally symmetric. There are relations,

$$\mathrm{Tr}(T_R^A T_R^B) = C(R)\delta^{AB} \,, \qquad f^{ABC} = -\frac{i}{C(R)} \mathrm{Tr}\left([T_R^A, T_R^B] T^C\right) \,, \tag{A.3}$$

where R denotes a representation. For the (anti-)fundamental representations, $\mathbf{N+3}$ and $\overline{\mathbf{N+3}}$, $C(R) = 1/2$. We also have

$$T_R^A T_R^A = C_2(R)\mathbf{1} \,, \qquad f^{ABC} f^{ABD} = (N+3)\delta^{CD} \,, \tag{A.4}$$

where $C_2(R)$ is the quadratic Casimir and $C_2(G) = N+3$ for the adjoint representation.

Next, let us divide the $SU(N+3)$ generators into the generators of the subgroups $U(1) \times SU(3) \times SU(N)$ and the other non-hermitian generators. We denote the $SU(3)$ generators as

$$T^a \,,\, T^b \,, \qquad a, b = 1, \cdots, 8 \,, \tag{A.5}$$

which satisfy

$$[T^a, T^b] = i f^{abc} T^c \,, \qquad f^{abc} f^{abd} = 3\delta^{cd} \,, \tag{A.6}$$

and the $U(1)$ generator as $T^9 \equiv \tilde{S}$. The $SU(N)$ generators are

$$T^m \,,\, T^n \,, \qquad m, n = 10 + 6N, \cdots, (N+3)^2 - 1 \,, \tag{A.7}$$

which satisfy

$$[T^m, T^n] = i f^{mnl} T^l \,, \qquad f^{mnl} f^{mnk} = N\delta^{lk} \,, \tag{A.8}$$

and the $6N$ non-hermitian generators are

$$T^p \,,\, T^{\bar{q}} \,, \qquad p, \bar{q} = 10, \cdots, 9 + 3N \,, \tag{A.9}$$

which satisfy

$$\mathrm{Tr}\,(T^p T^{\bar{q}}) = \frac{1}{2}\delta^{pq} \,, \tag{A.10}$$

for the fundamental representations. The commutation relations of the generators among the $SU(3)$, $U(1)$ and $SU(N)$ subgroups are zero,

$$[T^a, T^m] = [T^a, T^9] = [T^m, T^9] = 0 \,. \tag{A.11}$$

We also have

$$\begin{aligned} &\mathrm{Tr}\,(T^a T^m) = \mathrm{Tr}\left(T^a T^9\right) = \mathrm{Tr}\,(T^a T^p) = \mathrm{Tr}\,(T^a T^{\bar{p}}) \\ &= \mathrm{Tr}\left(T^m T^9\right) = \mathrm{Tr}\,(T^m T^p) = \mathrm{Tr}\,(T^m T^{\bar{p}}) = \mathrm{Tr}\left(T^9 T^p\right) = \mathrm{Tr}\left(T^9 T^{\bar{p}}\right) = 0 \,. \end{aligned} \tag{A.12}$$

and

$$f^{pqa} = f^{\bar{p}\bar{q}a} = 0 \,. \tag{A.13}$$

Then, we can derive the following useful formula,

$$\begin{aligned} f^{p\bar{q}a}(f^{p\bar{q}b})^* &= f^{\bar{q}pa}(f^{\bar{q}pb})^* \\ &= \frac{1}{2}\left(f^{ABa}f^{ABb} - f^{cda}f^{cdb}\right) \\ &= \frac{1}{2}\left((N+3)-3\right)\delta^{ab} = \frac{N}{2}\delta^{ab}\,. \end{aligned} \tag{A.14}$$

Note that $(f^{p\bar{q}a})^* = f^{\bar{p}qa}$. In the same way, we have

$$\begin{aligned} f^{p\bar{q}m}(f^{p\bar{q}n})^* &= f^{\bar{q}pm}(f^{\bar{q}pn})^* \\ &= \frac{1}{2}\left(f^{ABm}f^{ABn} - f^{klm}f^{kln}\right) \\ &= \frac{1}{2}\left((N+3)-N\right)\delta^{mn} = \frac{3}{2}\delta^{mn}\,. \end{aligned} \tag{A.15}$$

Note that $(f^{p\bar{q}m})^* = f^{\bar{p}qm}$.

B Summary of interactions

In this appendix, we summarize some of the interactions in the model.

B.1 Coloron interactions

We concentrate on the coloron interactions relevant to the coloron decays. The interaction which leads to $G' \to G_O G_O$ is given by

$$\mathcal{L} \supset \frac{g_H^2 - (g_3')^2}{\sqrt{g_H^2 + (g_3')^2}} f^{abc}(\partial^\mu G_O^a) G'^b_\mu G_O^c\,. \tag{B.1}$$

The relevant interaction of $G' \to G_O Z'$ is

$$\mathcal{L} \supset -\sqrt{\frac{2}{3}}\, m_{Z'} \sqrt{g_H^2 + (g_3')^2}\, G_O^a Z'_\mu G'^{\mu a}\,. \tag{B.2}$$

The interactions to give $G' \to X'\bar{X}'$ are

$$\begin{aligned} \mathcal{L} \supset \frac{g_H^2}{\sqrt{g_H^2 + (g_3')^2}} f^{ap\bar{q}} \Big\{ &- (\partial_\kappa G'^a_{\ \lambda}) X'^{\kappa p} \bar{X}'^{\lambda\bar{q}} + (\partial_\kappa X'^p_{\ \lambda}) G'^{\kappa a} \bar{X}'^{\lambda\bar{q}} - (\partial_\kappa X'^p_{\ \lambda}) \bar{X}'^{\kappa\bar{q}} G'^{\lambda a} \\ &+ (\partial_\kappa G'^a_{\ \lambda}) \bar{X}'^{\kappa\bar{q}} X'^{\lambda p} - (\partial_\kappa \bar{X}'^{\bar{q}}_{\ \lambda}) G'^{\kappa a} X'^{\lambda p} + (\partial_\kappa \bar{X}'^{\bar{q}}_{\ \lambda}) X'^{\kappa p} G'^{\lambda a} \Big\}\,. \end{aligned} \tag{B.3}$$

B.2 New massive gauge boson interactions

We here present the $X', \bar{X}'$ interactions which lead to the mixing between the scalar N-glueball and the singlet scalar G_S. The $X', \bar{X}'$ gauge boson interaction with the scalar G_S is given by

$$\mathcal{L} \supset \frac{1}{\sqrt{6}}\, g_H^2 a\, G_S X'_\mu \bar{X}'^\mu \,. \tag{B.4}$$

The cubic interactions of the $X', \bar{X}'$ gauge bosons with the $SU(N)_H$ gauge field H_μ^m are

$$\begin{aligned}\mathcal{L} \supset & - g_H f^{mp\bar{q}} (\partial_\kappa H_\lambda^m) X'^{\kappa p} \bar{X}'^{\lambda \bar{q}} + g_H f^{mp\bar{q}} (\partial_\kappa X'^p_\lambda) H^{\kappa m} \bar{X}'^{\lambda \bar{q}} - g_H f^{mp\bar{q}} (\partial_\kappa X'^p_\lambda) \bar{X}'^{\kappa \bar{q}} H^{\lambda m} \\ & + g_H f^{mp\bar{q}} (\partial_\kappa H_\lambda^m) \bar{X}'^{\kappa \bar{q}} X'^{\lambda p} - g_H f^{mp\bar{q}} (\partial_\kappa \bar{X}'^{\bar{q}}_\lambda) H^{\kappa m} X'^{\lambda p} + g_H f^{mp\bar{q}} (\partial_\kappa \bar{X}'^{\bar{q}}_\lambda) X'^{\kappa p} H^{\lambda m} \,.\end{aligned} \tag{B.5}$$

The quartic interactions are given by

$$\begin{aligned}\mathcal{L} \supset & - g_H^2 (f^{mnl} H_\kappa^m H_\lambda^n)(f^{p\bar{q}l} X'^{\kappa p} \bar{X}'^{\lambda \bar{q}}) \\ & - g_H^2 (f^{rm\bar{q}} H_\kappa^m \bar{X}'^{\bar{q}}_\lambda)(f^{\bar{r}np} H^{\kappa n} X'^{\lambda p}) \\ & + g_H^2 (f^{rm\bar{q}} H_\kappa^m \bar{X}'^{\bar{q}}_\lambda)(f^{\bar{r}np} X'^{\kappa p} H^{\lambda n}) \,.\end{aligned} \tag{B.6}$$

C The effective operator coefficients

We here identify the coefficients of the effective dimension eight operators presented in the main text, a_S, a_P, a_T, a_L and b_1, b_2. First, we have the relation,

$$\epsilon_{\mu\nu\rho\sigma}\epsilon_{\alpha\beta\gamma\delta} = -g_{\alpha\zeta} g_{\beta\eta} g_{\gamma\theta} g_{\delta\xi} \det \begin{pmatrix} \delta^\zeta_\rho & \delta^\zeta_\sigma & \delta^\zeta_\mu & \delta^\zeta_\nu \\ \delta^\eta_\rho & \delta^\eta_\sigma & \delta^\eta_\mu & \delta^\eta_\nu \\ \delta^\theta_\rho & \delta^\theta_\sigma & \delta^\theta_\mu & \delta^\theta_\nu \\ \delta^\xi_\rho & \delta^\xi_\sigma & \delta^\xi_\mu & \delta^\xi_\nu \end{pmatrix} \,. \tag{C.1}$$

Using this relation, the effective Lagrangian (4.3) can be rewritten as

$$\begin{aligned}
\mathcal{L}_{\rm eff} = \frac{g_H^2}{(4\pi)^2 m_{X'}^4}\Bigg\{ & \\
& \left(g_Y^2\chi_Y B_{\rho\sigma}B^{\rho\sigma} + g_s^2\chi_s \mathrm{Tr}\, G_{\rho\sigma}G^{\rho\sigma}\right)\left(a_S - \frac{1}{4}a_T + \frac{1}{3}a_L\right)\mathrm{Tr}\, F_{\alpha\beta}F^{\alpha\beta} \\
& + \left(g_Y^2\chi_Y B^{\mu\nu}B^{\rho\sigma} + g_s^2\chi_s \mathrm{Tr}\, G^{\mu\nu}G^{\rho\sigma}\right)\left(8a_P + \frac{2}{3}a_L\right)\mathrm{Tr}\, F_{\rho\mu}F_{\sigma\nu} \\
& - \left(g_Y^2\chi_Y B^{\mu\nu}B^{\rho\sigma} + g_s^2\chi_s \mathrm{Tr}\, G^{\mu\nu}G^{\rho\sigma}\right)\left(4a_P - \frac{2}{3}a_L\right)\mathrm{Tr}\, F_{\rho\sigma}F_{\mu\nu} \\
& + \left(g_Y^2\chi_Y B^{\mu}_{\ \sigma}B^{\rho\sigma} + g_s^2\chi_s \mathrm{Tr}\, G^{\mu}_{\ \sigma}G^{\rho\sigma}\right)(a_T - 2a_L)\,\mathrm{Tr}\, F_{\mu\lambda}F_{\rho}^{\ \lambda}\Bigg\} \\
& + \frac{g_H^3 g_Y}{(4\pi)^2 m_{X'}^4}\kappa_\Omega\left(b_1 B^{\mu\nu}\Omega^{(1)}_{\mu\nu} + b_2 B^{\mu\nu}\Omega^{(2)}_{\mu\nu}\right) .
\end{aligned} \tag{C.2}$$

The general expression of the effective Lagrangian has been calculated in [29, 30]. Using this result, we obtain

$$\begin{aligned}
a_S &= \frac{7}{288}(\gamma_1+\gamma_2) + \frac{1}{18}(\gamma_3+\gamma_4)\,, \qquad a_P = \frac{1}{288}(\gamma_1+\gamma_2) - \frac{1}{144}(\gamma_3+\gamma_4)\,, \\
a_T &= \frac{1}{8}(\gamma_1+\gamma_2) + \frac{1}{6}(\gamma_3+\gamma_4)\,, \qquad a_L = \frac{1}{48}(\gamma_1+\gamma_2) + \frac{1}{12}(\gamma_3+\gamma_4)\,, \\
b_1 &= \frac{1}{12}(\gamma_3+\gamma_4)\,, \qquad b_2 = \frac{1}{12}(\gamma_1+\gamma_2)\,,
\end{aligned} \tag{C.3}$$

where $(\gamma_1,\gamma_2,\gamma_3,\gamma_4) = \left(\frac{342}{35}, \frac{675}{105}, -\frac{621}{210}, -\frac{333}{420}\right)$ for a spin one particle integrated out. Then, we have the coefficients presented in (4.4).

References

[1] **ATLAS** Collaboration, G. Aad *et al.*, "Search for resonances in diphoton events with the ATLAS detector at $\sqrt{s} = 13$ TeV," `ATLAS-CONF-2016-018`.

[2] **CMS** Collaboration, V. Khachatryan *et al.*, "Search for new physics in high mass diphoton events in 3.3 fb^{-1} of proton-proton collisions at $\sqrt{s} = 13$ TeV and combined interpretation of searches at 8 TeV and 13 TeV," `CMS-PAS-EXO-16-018`.

[3] K. Harigaya and Y. Nomura, "Composite Models for the 750 GeV Diphoton Excess," *Phys. Lett.* **B754** (2016) 151–156, `arXiv:1512.04850 [hep-ph]`.

[4] Y. Nakai, R. Sato, and K. Tobioka, "Footprints of New Strong Dynamics via Anomaly and the 750 GeV Diphoton," *Phys. Rev. Lett.* **116** no. 15, (2016) 151802, arXiv:1512.04924 [hep-ph].

[5] R. Franceschini, G. F. Giudice, J. F. Kamenik, M. McCullough, A. Pomarol, R. Rattazzi, M. Redi, F. Riva, A. Strumia, and R. Torre, "What is the $\gamma\gamma$ resonance at 750 GeV?," *JHEP* **03** (2016) 144, arXiv:1512.04933 [hep-ph].

[6] N. Craig, P. Draper, C. Kilic, and S. Thomas, "Shedding Light on Diphoton Resonances," arXiv:1512.07733 [hep-ph].

[7] R. S. Chivukula, A. G. Cohen, and E. H. Simmons, "New strong interactions at the Tevatron?," *Phys. Lett.* **B380** (1996) 92–98, arXiv:hep-ph/9603311 [hep-ph].

[8] E. H. Simmons, "Coloron phenomenology," *Phys. Rev.* **D55** (1997) 1678–1683, arXiv:hep-ph/9608269 [hep-ph].

[9] Y. Bai and B. A. Dobrescu, "Heavy octets and Tevatron signals with three or four b jets," *JHEP* **07** (2011) 100, arXiv:1012.5814 [hep-ph].

[10] P. Langacker, "The Physics of Heavy Z' Gauge Bosons," *Rev. Mod. Phys.* **81** (2009) 1199–1228, arXiv:0801.1345 [hep-ph].

[11] C. J. Morningstar and M. J. Peardon, "The Glueball spectrum from an anisotropic lattice study," *Phys. Rev.* **D60** (1999) 034509, arXiv:hep-lat/9901004 [hep-lat].

[12] Y. Chen *et al.*, "Glueball spectrum and matrix elements on anisotropic lattices," *Phys. Rev.* **D73** (2006) 014516, arXiv:hep-lat/0510074 [hep-lat].

[13] R. L. Jaffe, K. Johnson, and Z. Ryzak, "Qualitative Features of the Glueball Spectrum," *Annals Phys.* **168** (1986) 344.

[14] M. E. Peskin and T. Takeuchi, "Estimation of oblique electroweak corrections," *Phys. Rev.* **D46** (1992) 381–409.

[15] R. Barbieri, A. Pomarol, R. Rattazzi, and A. Strumia, "Electroweak symmetry breaking after LEP-1 and LEP-2," *Nucl. Phys.* **B703** (2004) 127–146, arXiv:hep-ph/0405040 [hep-ph].

[16] **ATLAS** Collaboration, "Search for new phenomena in the dilepton final state using proton-proton collisions at $\sqrt{s} = 13$ TeV with the ATLAS detector," ATLAS-CONF-2015-070.

[17] **CMS** Collaboration, "Search for a Narrow Resonance Produced in 13 TeV pp Collisions Decaying to Electron Pair or Muon Pair Final States," CMS-PAS-EXO-15-005.

[18] **ATLAS** Collaboration, G. Aad *et al.*, "Search for new resonances in $W\gamma$ and $Z\gamma$ final states in pp collisions at $\sqrt{s} = 8$ TeV with the ATLAS detector," *Phys. Lett.* **B738** (2014) 428–447, arXiv:1407.8150 [hep-ex].

[19] **ATLAS** Collaboration, G. Aad *et al.*, "Search for high-mass dilepton resonances in pp collisions at $\sqrt{s} = 8$ TeV with the ATLAS detector," *Phys. Rev.* **D90** no. 5, (2014) 052005, arXiv:1405.4123 [hep-ex].

[20] R. S. Chivukula, A. Farzinnia, J. Ren, and E. H. Simmons, "Hadron Collider Production of Massive Color-Octet Vector Bosons at Next-to-Leading Order," *Phys. Rev.* **D87** no. 9, (2013) 094011, arXiv:1303.1120 [hep-ph].

[21] R. S. Chivukula, A. Farzinnia, E. H. Simmons, and R. Foadi, "Production of Massive Color-Octet Vector Bosons at Next-to-Leading Order," *Phys. Rev.* **D85** (2012) 054005, arXiv:1111.7261 [hep-ph].

[22] **CMS** Collaboration, V. Khachatryan *et al.*, "Search for quark contact interactions and extra spatial dimensions using dijet angular distributions in proton-proton collisions at $\sqrt{s} = 8$ TeV," *Phys. Lett.* **B746** (2015) 79–99, arXiv:1411.2646 [hep-ex].

[23] K. Hagiwara and K. Hikasa, "Searches for quark and lepton composites: in Review of Particle Physics (RPP 1998)," *Eur. Phys. J.* **C3** (1998) 772–774.

[24] E. Eichten, I. Hinchliffe, K. D. Lane, and C. Quigg, "Super Collider Physics," *Rev. Mod. Phys.* **56** (1984) 579–707. [Addendum: Rev. Mod. Phys.58,1065(1986)].

[25] L. J. Hall, "Grand Unification of Effective Gauge Theories," *Nucl. Phys.* **B178** (1981) 75–124.

[26] S. Weinberg, "Effective Gauge Theories," *Phys. Lett.* **B91** (1980) 51–55.

[27] M. J. Strassler and K. M. Zurek, "Echoes of a hidden valley at hadron colliders," *Phys. Lett.* **B651** (2007) 374–379, arXiv:hep-ph/0604261 [hep-ph].

[28] J. E. Juknevich, D. Melnikov, and M. J. Strassler, "A Pure-Glue Hidden Valley I. States and Decays," *JHEP* **07** (2009) 055, arXiv:0903.0883 [hep-ph].

[29] R. R. Metsaev and A. A. Tseytlin, "ON LOOP CORRECTIONS TO STRING THEORY EFFECTIVE ACTIONS," *Nucl. Phys.* **B298** (1988) 109.

[30] S. Fichet and G. von Gersdorff, "Anomalous gauge couplings from composite Higgs and warped extra dimensions," *JHEP* **03** (2014) 102, arXiv:1311.6815 [hep-ph].

[31] **ATLAS** Collaboration, G. Aad *et al.*, "Search for an additional, heavy Higgs boson in the $H \to ZZ$ decay channel at $\sqrt{s} = 8$ TeV in pp collision data with the ATLAS detector," *Eur. Phys. J.* **C76** no. 1, (2016) 45, arXiv:1507.05930 [hep-ex].

[32] H. M. Georgi, S. L. Glashow, M. E. Machacek, and D. V. Nanopoulos, "Higgs Bosons from Two Gluon Annihilation in Proton Proton Collisions," *Phys. Rev. Lett.* **40** (1978) 692.

[33] R. N. Cahn and S. Dawson, "Production of Very Massive Higgs Bosons," *Phys. Lett.* **B136** (1984) 196. [Erratum: Phys. Lett.B138,464(1984)].

[34] A. D. Martin, W. J. Stirling, R. S. Thorne, and G. Watt, "Parton distributions for the LHC," *Eur. Phys. J.* **C63** (2009) 189–285, arXiv:0901.0002 [hep-ph].